

LINEAR AND NONLINEAR ASPECTS OF CLIMATE RESPONSE TO EXTERNAL FORCINGS

A. V. Eliseev^{1,2,3*}

UDC 551.511

The main role in the current climate change is played by anthropogenic forcings, primarily anthropogenic emissions of greenhouse gases and aerosols. On the global scale, the response of the Earth system to these forcings is close to linear. In particular, it depends mostly on the magnitude of such forcings and only weakly on their nature and spatial localization. However, even with relatively small (in absolute value) external forcings, the response of the characteristics of the Earth system can be essentially nonlinear with the manifestation of tipping points, upon transition through which the behavior of the Earth's climate changes qualitatively. Examples are given for linear and nonlinear mechanisms of the climate response to external forcings.

1. INTRODUCTION

Analysis of the causes and consequences of climate change is one of the main tasks of modern geophysics. Combining the problems of hydrodynamics, thermodynamics, propagation of waves of various nature, the theory of plasticity, physical chemistry, solid state physics, radiophysics and biophysics, and physical climatology now firmly occupies a place among the physical sciences. Moreover, the practical importance of understanding the causes of climate changes and their prediction links physical climatology with a number of other disciplines such as geography, biology, and even economics, sociology, and medicine.

According to the recently published Sixth Assessment Report (AR6) of Intergovernmental Panel on Climate Change (IPCC) [1], the last decades of the 20th century and the first decades of the 21st century have witnessed an unprecedented rate of climate change. In particular, the linear trend of the globally averaged surface temperature T_g averaged over the datasets used in IPCC AR6 for 1880–2020 was 1.1 K, including 1.0 K for 1960–2020. Thus, the average growth rate of T_g for the indicated time intervals is close to 0.08 K/decade and 0.25 K/decade, respectively. The average value of T_g for 2010–2019 years turns out to be higher than for any time interval in the last 125 thousand years since the last interglacial.

Herein, the content of CO₂ in the atmosphere reached 412 ppmv on average for 2020. This value is also unprecedentedly high, for at least the last 2 million years.

The purpose of this paper is to review current climate change in the context of the corresponding variations on a larger time scale from 10³ to 10⁵ years, causes and consequences of the occurring climate change, as well as linear and nonlinear mechanisms for the formation of a climate response to external forcings.

* eliseev.alexey.v@mail.ru

¹ M. V. Lomonosov State University of Moscow; ² A. M. Obukhov Institute of Atmospheric Physics of the Russian Academy of Sciences, Moscow; ³ Kazan (Volga) Federal University, Kazan, Russia. Translated from *Izvestiya Vysshikh Uchebnykh Zavedenii, Radiofizika*, Vol. 66, Nos. 2–3, pp. 87–103, February–March 2023. Russian DOI: 10.52452/00213462_2023_66_02_87 Original article submitted December 29, 2022; accepted March 31, 2023.

2. CLIMATE CHANGE OVER THE INDUSTRIAL PERIOD

In the IPCC Sixth Assessment Report AR6 [1] based on an analysis of extensive empirical material and results of calculations with numerical Earth system models the following conclusions on climate change over the industrial period have been drawn: 66% confidence interval (CI66) for global temperature increase at the surface in 2010–2019 compared with 1850–1900, is from 0.9 up to 1.2 K, according to observational data. The corresponding CI66 for CMIP6 (Coupled Models Intercomparison Project, phase 6) model generation is consistent with an empirical estimate, ranging from 0.8 to 1.3 K.

Climate warming is accompanied by an increase in precipitation on the land of the Northern hemisphere at the middle and high latitudes with enhanced contrast of precipitation between the humid tropics and the dry subtropics. However, summer monsoon rainfall on land from the 1950s to the 1980s generally decreased. In addition, after 1979, precipitation increased in summer at high latitudes of the Southern hemisphere and decreased at the midlatitudes of this hemisphere. Changes in precipitation in the Southern Hemisphere are due to natural variability of climate.

More frequent heat waves and rarer manifestations of cold waves are revealed.

Along with the increase in the content of CO₂ noted in the Introduction, the content of other greenhouse gases for which anthropogenic emissions are significant, such as methane CH₄ and nitrous oxide N₂O, have increased many times compared with the preindustrial level: their content in 2019 reached 1866 ppbv and 332 ppbv, respectively.

Climate warming is accompanied by melting sea ice in the Arctic since the late 1970s. The decrease in the area and thickness of sea ice cover is reproduced in all CMIP6 models over the past decades, although these models do not show a small observed increase in the area of sea ice in Antarctica during the same period.

Since the middle of the 20th century, there has been a decrease in snow cover in the Northern hemisphere in spring and also an almost ubiquitous retreat of glaciers in recent decades. In the last two decades, there is also an intense mass loss of the Greenland ice sheet and, to a lesser extent, the Antarctic ice sheet.

Ocean heat content is increasing, at least since the 1970s, including in layers deeper than 700 m.

Global ocean level (closely related to its heat content) increased by 20 cm (CI66 from 15 to 25 cm) for 1901–2018. The speed of sea level rise increased from 1.3 mm/year (CI66 from 0.6 to 2.1 mm/year) on average for 1901–1971 up to 1.9 mm/year (CI66 from 0.8 to 2.9 mm/year) on average for 1971–2006 and up to 3.7 mm/year (CI66 from 3.2 to 4.2 mm/year) on average for 2006–2018.

Changes in the state of the biosphere are consistent with observed climate warming: bioclimatic zones have shifted towards the poles both in the Northern and Southern hemispheres, and the growing season has lengthened (since the 1950s the average speed of this elongation at the middle and subpolar latitudes of the Northern hemisphere was 2 days/decade).

3. CAUSES OF THE CURRENT CLIMATE CHANGE

A quantitative characteristic of external (including anthropogenic) forcing on the Earth system is the radiative forcing. This characteristic is defined as the change in energy fluxes at the nominal top of the atmosphere when a radiatively active substance such as greenhouse gases or aerosols is added to the Earth system, while the state of the latter remains unchanged. Quantitatively, the radiative forcing R can be expressed as a non-autonomous term on the right-hand side of the equation of energy conservation in the Earth system:

$$dH/dt = R + F, \quad (1)$$

where H is the heat content of the system, t is the time, and the term F characterizes the adjustment of the system and feedback in it (definitions of both terms are given in Sec. 5.1).

It should be noted that the use of the nominal top of the atmosphere to determine the radiative forcing is due to the fact that the energy balance at this altitude has the simplest physical structure and

does not include fluxes of sensible and latent heat. Depending on the climate model and description details (see Sec. 5.1), this bound can extend from the tropopause to an altitude from which the inhomogeneity of the molecular atmospheric mass due to the effect of ultraviolet radiation on dissociation of polyatomic molecules (starting from approximately 120 km) begins to be manifested.

The analysis of radiative forcing in various papers is usually performed using detailed line-by-line models of radiation energy transfer in the atmosphere (i. e., models in which such a process is calculated with a very high spectral resolution), making it possible to allow for the contribution of individual lines of absorption or scattering on the radiation energy transfer and empirical data (as well as model ones in the absence of the latter) on the state of the atmosphere (its chemical composition, characteristics of cloudiness, and temperature structure; see e. g., [2]). Such an approach in combination with data on the intensity of anthropogenic forcing on the Earth system and variations in natural forcings on climate (changes in the energy flux from the Sun at the top bound of the atmosphere and the effect of volcanic eruptions on the composition of the stratosphere) have led to the following conclusions in IPCC AR6 [1].

Change in anthropogenic radiative forcing R over the industrial era (1750–2019) amounted to 2.7 W/m^2 with CI66 from 2.0 to 3.5 W/m^2 .

The contribution of anthropogenic emissions of greenhouse gases and their chemical predecessors in this R value is 3.8 W/m^2 with CI66 from 3.5 to 4.2 W/m^2 . In turn, the radiative forcing of greenhouse gases includes CO_2 (2.2 W/m^2 with CI66 from 1.9 to 2.4 W/m^2), CH_4 (0.5 W/m^2 with CI66 from 0.4 to 0.6 W/m^2), halogenated substances (0.4 W/m^2 with CI66 from 0.3 to 0.5 W/m^2), and N_2O (around 0.2 W/m^2).

This radiative forcing is partially compensated by the cooling effect of atmospheric aerosols (-1.3 W/m^2 with CI66 from -0.6 to -2.0 W/m^2), mostly due to their interaction with the clouds (effect on the size of cloud drops and crystals; -1.0 W/m^2 with CI66 from -0.3 to -1.7 W/m^2). The rest is due to the direct effect of aerosols on scattering and absorption of radiation in the atmosphere (-0.3 W/m^2 with CI66 from 0.0 to -0.6 W/m^2).

Natural climate variability is an important climate-forming process. The Earth system is capable of forming quasi-oscillatory processes, including those with time scales of several decades or more [3, 4]. Such processes appear even at the global level, with an even greater role on subcontinental and smaller spatial scales [5]. The contribution of natural variability to the ongoing climate change depends on the time interval with a specific sign of temperature anomalies. In particular, natural climatic variability is the cause of the so-called warming pause from the end of 1990s to the middle of 2010s, when the rate of warming of the Earth system has significantly decreased compared to the 1980s and most of the 1900s and compared to the time interval from the mid-2010s. In this case, the natural variability manifested itself as variations in the intensity of heat absorption by the ocean [6]. It also causes a temporary cooling of the climate in the 1960s and 1970s [7]. Extraction of the contribution of natural variability and response to external forcings in the ongoing climate change is one of the main problems of modern physical climatology. Methods of statistical analysis of time series, including radiophysical methods, are intensely used to solve this problem. According to IPCC AR6 estimates, the contribution of natural climate variability to climate change in 1850–2019 ranges from -0.2 to $+0.2 \text{ K}$.

The IPCC AR6 clearly states that the anthropogenic impact is exactly the main driver of climate warming since the pre-industrial period. In particular (see Fig. 1), the following is shown.

The total forced (i. e., related to external forcings on the Earth system) change in globally averaged surface temperature in 1750–2019 (note that the Introduction contains values for a different time interval) was 1.3 K with CI66 from 1.0 to 1.7 K .

This change includes heating due to the accumulation of well-mixed greenhouse gases in the atmosphere (1.0 K with CI66 from 1.2 to 2.2 K), heating due to an increase in the ozone content in the troposphere (0.2 K with CI66 from 0.1 to 0.4 K), cooling due to the effect of atmospheric aerosols (-0.6 K with CI66 from -0.2 to -1.0 K), and cooling due to surface albedo variations during land use and heating during the deposition of soot aerosol on snow (the total effect of the last two processes is cooling and is equal to -0.1 K with CI66 from -0.2 to $+0.0 \text{ K}$); see also [8].

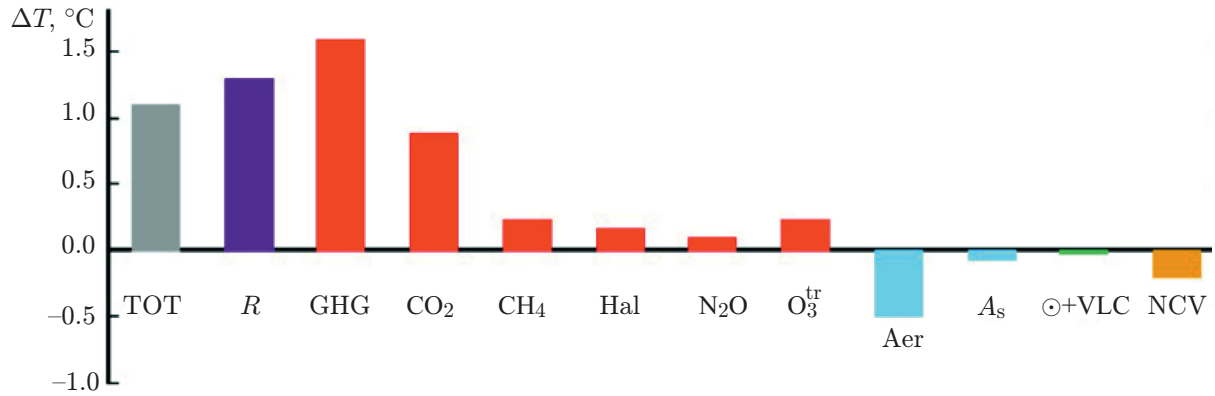


Fig. 1. Central estimates for the absolute contribution of various processes to climate change in 1750–2019 according to IPCC AR6 data. From left to right: all processes (TOT), all radiative forcings (R), all greenhouse gases (GHG), carbon dioxide (CO_2), methane (CH_4), halogens (Hal), nitrous oxide (N_2O), tropospheric ozone (O_3^{tr}), tropospheric aerosols (Aer), Earth’s surface albedo change (A_s), solar and volcanic activity ($\odot+\text{VLC}$), and natural climate variability (NCV).

The response of the global surface temperature to the above natural forcings is only from -0.1 K to $+0.1$ K.

It should be specially noted that, despite a number of statements about the role of natural external forcings in the ongoing climate change (a review and critique of these papers are available in [9]), quantitative reproduction of T_g variations in the 20th century is currently impossible without taking into account anthropogenic impacts on climate (Fig. 2).

The general increase in the moisture content of the atmosphere during warming leads to a general increase in precipitation variability with more frequent shower (convective) precipitation and a decrease in continuous precipitation (related to large-scale condensation) [10]. In this case, monthly average precipitation increases in the tropics and in the middle and subpolar regions (already now characterized by excessive moisture) and decreases in dry subtropics [1]. In addition, IPCC AR6 noted the role of anthropogenic atmospheric aerosols in the reduction of summer monsoon rainfall on land from the 1950s to the 1980s.

At the same time, temperature variability does not appear during warming: standard deviation of interannual temperature variations in the middle and subpolar latitudes decreases on the whole, while in others it does not change significantly [11, 12, 13, 14].

4. LINEAR COMPONENT OF CLIMATE RESPONSE TO EXTERNAL FORCINGS

The linear component of the response can be obtained by representing the term F in (1) in the form

$$F = \lambda \Delta T, \quad (2)$$

where ΔT is the surface temperature variation relative to pre-industrial values, and $\lambda = \text{const} < 0$ is called the climate feedback parameter. This name is due to the fact that for the equilibrium response to a given stationary radiative forcing R we have

$$\Delta T_{\text{eq}} = -R/\lambda. \quad (3)$$

Equation (2) assumes universality of the vertical structure of response to various external forcings.

For CMIP6 ensemble models, $\lambda = -(0.59\text{--}1.71) \text{ W}/(\text{m}^2 \cdot \text{K})$ with an ensemble-average value of $-0.95 \text{ W}/(\text{m}^2 \cdot \text{K})$ [15, 16]. When the CO_2 content in the atmosphere (q_{CO_2}) is doubled, radiative forcing is close to $3.7 \pm 0.4 \text{ W}/\text{m}^2$ and such an interval of λ corresponds to an equilibrium climate sensitivity of 1.8 to 5.7 K for doubled q_{CO_2} .

Herein, the response of the troposphere to external forcings is to a large extent linear, both globally and regionally. In particular, the spatial structure of variations in the main climatic variables (e. g., surface

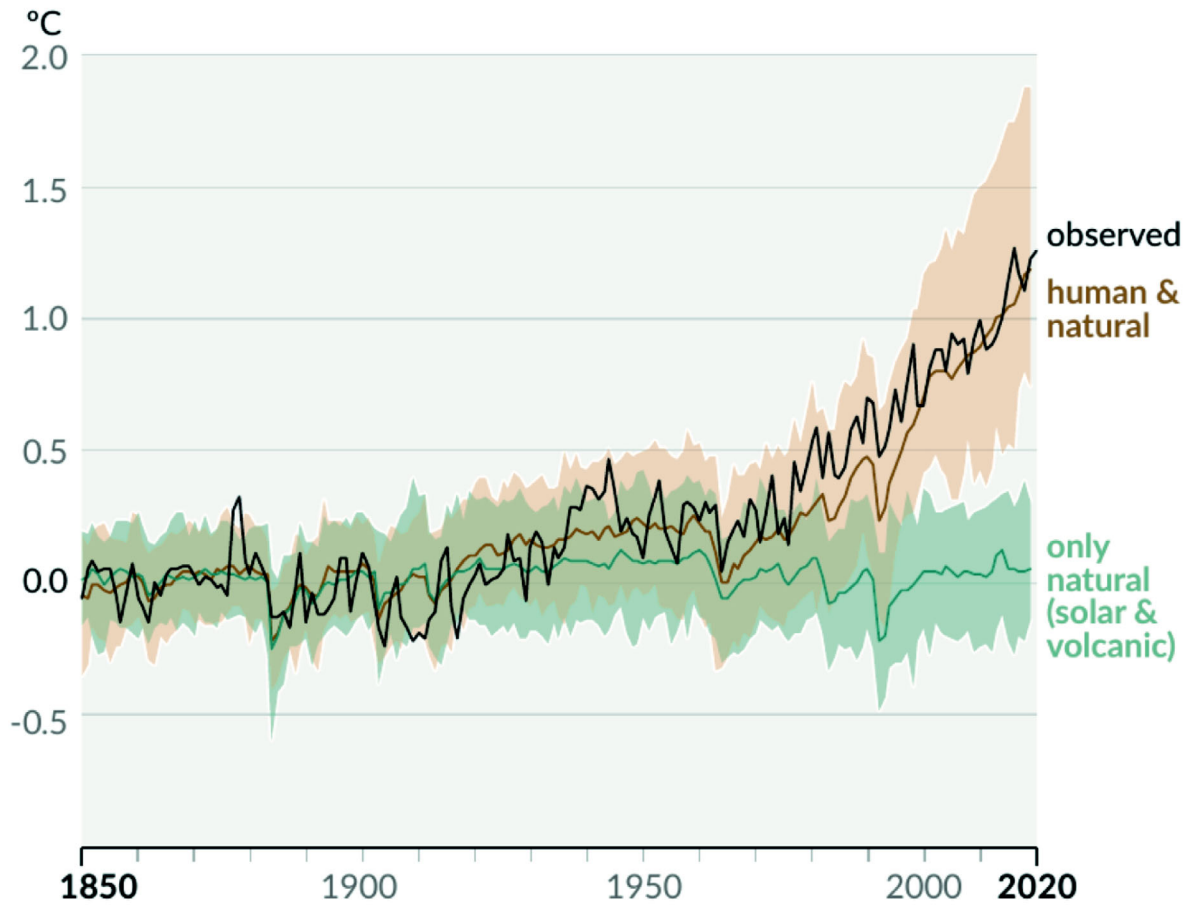


Fig. 2. Global surface temperature change in 1850–2019 based on CMIP6 (Coupled Models Intercomparison Project, phase 6) models in calculations taking into account only natural impacts on climate (only natural (“solar & volcanic”)) and taking into account natural and anthropogenic impacts on the Earth system (“human & natural”) in comparison with observational data (“observed”). Filled area of the corresponding color shows the intermodel standard deviation for the indicated numerical experiments. Reproduced from [1, Fig. SPM.1b].

temperature or precipitation), when reduced to a single variation in global temperature, differs little between different models. Moreover, it differs little among different types of external forcing with a fundamentally different horizontal localization of the radiative forcing.

A numerical estimate of the degree of linearity of the climate response will be given in Sec. 5.1.

In a linear approximation, the individual processes that form the climate response and contribute to the parameter λ can be considered mutually independent. In such a case [17],

$$\lambda = \sum_i \lambda_i, \quad (4)$$

where the subscript i indicates individual climate feedbacks. Contribution of individual feedbacks is scaled by the so-called Planck response, namely, the response of the Earth as an absolutely black body, for which the variation in T_g due to the radiative forcing R is equal to $\Delta T_{\text{Planck}} = R / (4\sigma T_0^3)$, so that $\lambda_{\text{Planck}} = -4\sigma T_0^3$. Here, T_0 is the value of T_g before the occurrence of the indicated radiative forcing and σ is a Stefan — Boltzmann constant.

The main feedbacks in the Earth system, in addition to the Planck one, are the following (Fig. 3).

1) Feedback related to responses to atmospheric water vapor content and lapse rate. During climate warming (for definiteness) in the case of a small variation in relative humidity [18], according to the Clausius — Clapeyron relation, an increase in the content of atmospheric water vapor as the strongest greenhouse

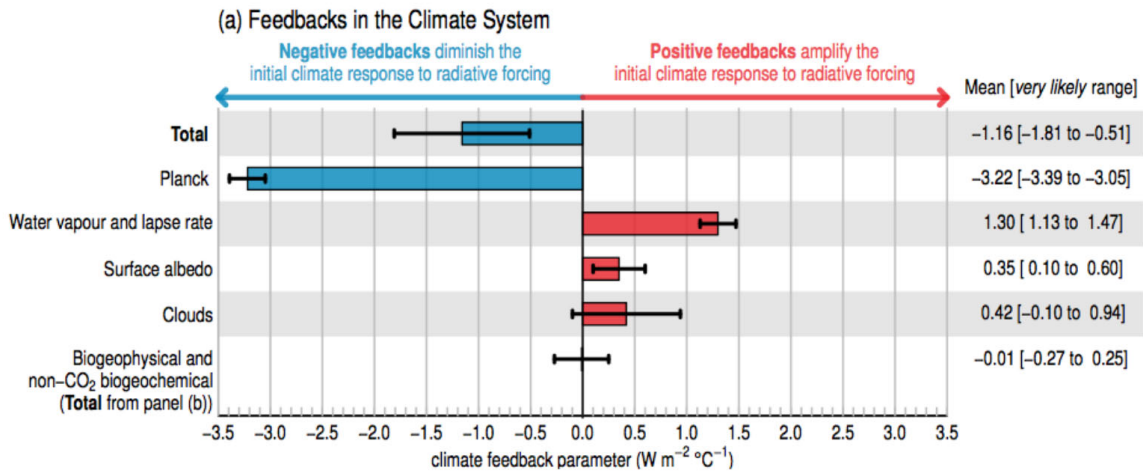


Fig. 3. Major climate feedbacks. On the right are median estimates and confidence intervals 5–95%. Here, total is the total feedback, Planck is the Planck feedback, water vapor and lapse rate is the feedback related to water vapor content responses in the atmosphere and lapse rate, surface albedo is the feedback related to the Earth’s surface albedo response, clouds is the feedback related to clouds, and biogeophysical and non-CO₂ biogeochemical is the feedbacks related to biogeophysical and biogeochemical processes. Reproduced from [1, Fig. TS.17a].

gas and solar radiation absorber should be expected. This leads to heating of the troposphere. However, an increase in water vapor content also causes a decrease in lapse rate (this is the wet adiabatic lapse rate). This leads to a higher temperature at the “radiation level” (the altitude of which is related to the total amount of greenhouse gases in the atmosphere) and, consequently, a more intensive loss of energy of the climate system due to radiation. In view of the close relationship between these feedbacks, they are combined into one, which also narrows the intensity uncertainty interval of this feedback [18]. In absolute value, the parameter of this combined feedback is about 1/3 of the Planck response.

2) Feedback related to variations in the Earth’s surface albedo due to variations in the area of spread of snow (as well as glaciers) on land and sea ice. In absolute value, the median estimate for the parameter of this feedback is about 1/8 of the Planck response.

3) Feedback related to variations in cloud characteristics (cloud fraction, altitude extent, total water content in clouds and phase composition of water). It has been found that an increase in the altitude of the upper bound of the clouds promotes the greenhouse effect, while an increase in total water content in cloudiness in the lower troposphere leads to cooling of the climate [19]. Accordingly, an increase in the cloud fraction in the lower (upper) troposphere leads to cooling (heating) of the climate. Apparently, among the clouds of the lower troposphere, clouds in the oceanic boundary layer of the subtropics have an especially strong effect on equilibrium climate sensitivity to doubled q_{CO_2} [20, 21]. Adequate reproduction of such clouds by models requires a very high vertical resolution in the lower troposphere. For a currently available vertical resolution of climate models, response of these clouds to climate change differs fundamentally among models. Besides, a number of climate feedbacks related to the effect of cloudiness on precipitation (and, therefore, on the general hydrological cycle), as well as on the lightning activity [22] is known. Median estimate of the total strength of feedback due to cloudiness is close to 1/8 of the Planck response.

4) Feedbacks related to biogeophysical and biogeochemical processes. They arise as a result of the response of biogeochemical cycles to climate changes, as well as due to the direct impact of q_{CO_2} on the intensity of photosynthesis [23, 24]. In IPCC AR6, their contribution is estimated as small, but integrally they are able to increase the response of the Earth system for given emissions of well-mixed greenhouse gases by about 10% [23]. The cause of occurrence of biogeophysical feedbacks is the dependence of the surface albedo and the transfer of moisture from the soil to the atmosphere on the state of the terrestrial vegetation.

Summarily, climate feedbacks enhance the Earth system response to external forcings by a factor of 3.0 to 3.5 (median estimate) relative to the Planck response.

5. FEEDBACKS AND ADJUSTMENT OF THE RESPONSE OF THE EARTH SYSTEM COMPONENTS UNDER EXTERNAL FORCING

5.1. Adjustment of the climate state to the radiative forcings

Despite the general linearity of the troposphere response to external forcing on large spatiotemporal scales (Sec. 4), the nonlinear component of the response is also of fundamental importance.

Such a nonlinearity has been noted even at the global level. In particular, identical radiative forcings due to the doubled q_{CO_2} and because of the solar constant increase by 2% lead to close responses in the troposphere, but responses differing even in sign in the stratosphere [25]. The physical reason for this is the difference in the impact of these effects on the vertical structure of the fluxes of radiant energy in the atmosphere. With the increase in q_{CO_2} (as well as in the content of any other greenhouse gas in the atmosphere), radiation coming from below in the thermal range is absorbed, followed by its re-emission both up and down, that is, the energy is locked below a certain altitude in the atmosphere. Herein, the atmosphere is heated up below this altitude and cooled above it. With the increase in the total solar irradiance, in turn, there is heating of all layers of the Earth system where radiant energy in the solar range comes. As a consequence, the difference in the vertical structure of the climate response between these two forcings is one of the important arguments of the dominant contribution of anthropogenic impact to climate change in recent decades, since warming of the troposphere is accompanied by cooling of the stratosphere, according to observational data [1].

In connection with such a difference in the stratosphere response to radiative forcings of various nature, it was proposed to calculate them at the level of the tropopause and use not instantaneous values, but the value after the stratosphere adjustment [25], which for the forcing with horizontal scale from 10^3 km is of radiative (rather than circulation) nature and occurs within a year [26] (Fig. 1). Such a definition of radiative forcing was named adjusted forcing R_a . However, later the nonlinearity of the troposphere response to adjusted forcing [27] was revealed. In connection with this, the concept of effective radiative forcing R_s was introduced, which is currently used when evaluating the parameter λ and its components [1]. Technically, the effective forcing R_s can be calculated by using climate models at a fixed temperature of the Earth's surface [27].

Note that the concept of the Earth system adjustment, introduced in the previous paragraph, is different from the concept of climate response. According to the IPCC AR6 definition (Sec. 8.3.1 of [1]) the adjustment processes include a change in the state of the system that occurs at a fixed surface temperature. Due to the close relationship between the thermal state of the surface and the state of the troposphere [28], only a relatively small change in the atmosphere state is possible in this case.

In advanced climate models, rigorous schemes of numerical experiments with a fixed surface temperature are not possible, and only the temperature of the ocean surface can be fixed. Surface temperature of land, glaciers, ice sheets, and sea ice interactively responds a change in the atmosphere state. Despite the relative smallness of this response on scales of up to several years (see the text below), this leads to ambiguity in the definitions of adjustment of the Earth system to external forcing and climate response to such an impact.

The main role in the adjustment of the Earth system for the CMIP6 ensemble models is played by the adjustment of temperatures of the troposphere and stratosphere, water vapor content in the troposphere, and cloudiness characteristics [29]. Herein, the features of adjustment of cloudiness characteristics to radiative forcing differ significantly among different climate models.

Time scale for adjusting the troposphere state to radiative forcing can reach several years [29]. On this time scale, a climate response to this impact already starts to form. This additionally increases the mentioned ambiguity in separating the troposphere state variation into adjustment and response and, therefore, leads to

ambiguity in determining the effective radiative forcing. However, it should be borne in mind that for impacts with a planetary horizontal scale (well-mixed greenhouse gases, stratospheric ozone, stratospheric aerosols, energy flux from the Sun, changes in the parameters of the Earth’s orbit), the difference between R_a and R_s is small. It becomes important for forcings with a strong horizontal inhomogeneity such as tropospheric aerosols, land use or tropospheric ozone [27].

5.2. Formation of the Earth system response to external forcing

Dependence of the climate response on the type of external forcing (with various spatial structure) can be quantitatively characterized in terms of the radiative forcing efficacy [27]. This quantity is defined as the temperature response to a given radiative forcing relative to the corresponding response to the change in q_{CO_2} of the same magnitude and sign. For most external forcings on the global level, efficacies range from 0.9 to 1.1 [27]. Thus, the linear component of the response on the global level describes about 90% of the response of the Earth system. Tropospheric aerosols, primarily carbon ones, for which the efficacy can reach 1.25, are the exception. Note, however, that the ambiguity of the definition of effective radiative forcing also leads to ambiguity in determining the efficacy.

The nonlinearity of the response of the Earth system to external forcings manifests itself in the dependence of the parameter λ on the conditions of a numerical experiment with a model and on the time within the framework of this numerical experiment. In particular, the dependence of λ on time was revealed in [30, 31]. This change is related to the response of the cloudiness characteristics to external forcing. This is due partly to the adjustment of the Earth system to forcings. However, the component of this change with a centenary time scale cannot be considered an adjustment. The change in the cloudiness response on this time scale is related to slow (on a time scale of up to one and a half millennia [32, 33, 34]) response of global ocean circulation to external forcing.

In addition, the dependence of the parameter λ on the climate state was revealed. This, in particular, manifests itself in the dependence of λ on the sign of external forcing with a sufficiently large absolute value of the latter. For example, [35] notes that in three of the four analyzed models of the Earth system the absolute value of this parameter when q_{CO_2} is doubled is less (and, consequently, the surface temperature response is greater) than during the transition from pre-industrial Holocene to the last ice age. A temperature response increase under forcing leading to greater climate warming was also noted in [36], where it was related with an exponential increase in the atmospheric water vapor content during warming (see Sec. 4). Finally, paleoreconstruction [37] for the temperature optimum of the Paleocene–Eocene boundary (56 million years ago; this is the warmest period for the last 60 million years) corresponds to an equilibrium climate sensitivity of 5.7 to 7.4 °C for doubled q_{CO_2} , which exceeds the sensitivity of all advanced models (Sec. 3). Note, however, that [37] does not take into account the radiative forcing of well-mixed greenhouse gases other than CO_2 , primarily methane, the release of which into the atmosphere is currently considered the main cause of the temperature optimum 56 million years ago [24].

The nonlinearity of the response of the Earth system also manifests itself in the same signs of changes in the characteristics of atmospheric circulation both during global warming and global cooling. In particular, simplified models of atmospheric circulation noted the maximum eddy kinetic energy for the synoptic time scale interval (from 2 to 7 days) [38] and a minimum (in terms of area covered at the Earth’s surface) for eddy activity on a larger intra-seasonal scale (up to 1 month; this corresponds to the development of atmospheric blockings) [39]. The manifestation of this nonmonotonicity in more detailed models of the Earth system and its relationship with the dependence of λ values on the climate state are currently not revealed.

5.3. Tipping points during changes in the state of the Earth system

Tipping points are another manifestation of the nonlinearity of the climate response to external forcings. According to the IPCC AR6 glossary, they are defined as threshold states of the Earth system, upon passing through which the behavior of the latter changes qualitatively. In [40], for a system with a

state vector \mathbf{Y} and a set of govern parameters \mathbf{p} a classification is proposed, which includes three types of tipping points. The first type (type B tipping points) is the so-called bifurcation tipping points, when the transition through a bifurcation point occurs as \mathbf{p} is changed. Exit of the trajectory of the system from the attraction domain of an attractor due to the random noise effect corresponds to a type N tipping point. The third type (type R tipping points) corresponds to the case where with a sufficiently fast change in the parameter \mathbf{p} with respective deformation of the attractor and its domain of attraction the trajectory of the system is outside this domain. Type R tipping points are characterized by the mutual relation between the rates of change $\|d\mathbf{Y}/dt\|$ and $\|d\mathbf{p}/dt\|$, where t is the time and $\|\mathbf{a}\|$ is the norm of the vector \mathbf{a} in the functional space to which the trajectories belong.

Tipping points of all types are possible even in the simplest climate models. A bifurcation tipping point in the energy balance climate model with the solar climate change was revealed by M. I. Budyko [41]. Examples of tipping points of other types are given in [40]. One example of manifestation of a type R tipping point is a model for the development of an ozone hole with increasing chlorine content in the stratosphere of the Antarctic [42, 43].

Important characteristics of tipping points are the threshold value of \mathbf{p} , at which the behavior of the system changes qualitatively (except for type N tipping points) and the time scale of the development of a new trajectory system in the supercritical region.

The best-known tipping points in climate are the possible collapse of meridional circulation of the ocean (ocean conveyor) in the case of rapid freshening of the North Atlantic and the possible death of the Amazonian forests during the development of arid conditions in the Amazon basin with further climate warming [44, 45]. The control parameter for the first tipping point is the intensity of fresh water input to the North Atlantic and the level of the global climate warming for the second one. Herein, the threshold values of the control parameters for both tipping points are poorly known [44, 45]. After passing through the bifurcation threshold, the development of a significant deviation of the trajectory from the prebifurcation one for the first tipping point even after a very fast and strong freshening of the North Atlantic (which in itself is unlikely with the further warming due to the slow melting of the Greenland ice sheet—the only reservoir with a sufficient mass of fresh water in this region) requires at least several hundred years [46]. For the bifurcation point related to the death of Amazonian forests, this time scale is of the order of several decades [1].

Another reason for the occurrence of a tipping point is the possible release of methane into the atmosphere from shelf methane hydrates under further climate warming [1]. However, the time scale of its development is at least some millennia [47, 48], which, with allowance for a much smaller time scale of anthropogenic impact and methane loss for oxidation in the water column, makes significant CH_4 emissions from this source unlikely.

Discussion of other possible tipping points is available in [44, 45]. As for the mentioned tipping points, the climatic thresholds for their activation are poorly known. In connection with this, IPCC AR6 only stated an increase in the probability of occurrence of these points with increasing deviation of the climate from the current one. For models of the CMIP6 ensemble, they manifest themselves mainly in the melting of ground permafrost with the release of greenhouse gases from it (from the substrate, which formed during the Pleistocene glaciations and before its melting was excluded from the global biogeochemical cycles). The intensity of related feedbacks is taken into account among biogeophysical and biogeochemical feedbacks and is therefore relatively low (see Sec. 4).

A review of tipping points known from paleoclimate changes is given in [49]. It was noted that the development of a climate anomaly due to the activation of a tipping point may lead to the activation of another tipping point, i. e., a cascade effect (see also [50, 51]). On the other hand, the inertia of the climate allows a temporary transition (with a duration less than or of the order of magnitude of the time scale of anomaly development in the supercritical region) without a final exit from the domain of attraction of a modern climate attractor.

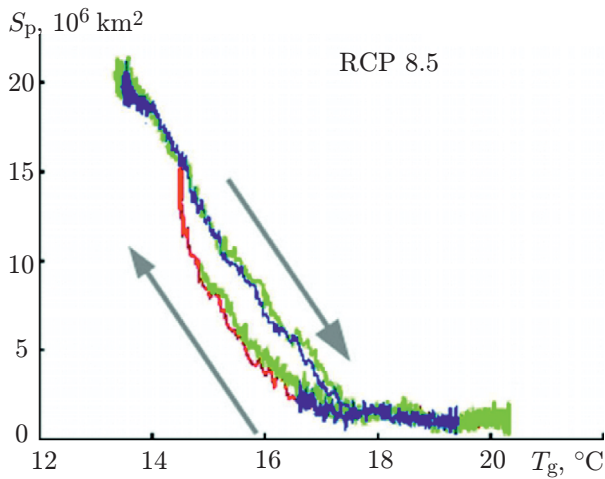


Fig. 4. Extent area of near-surface permafrost soils S_p as a function of the globally averaged annual surface temperature T_g according to calculations using the Earth system model of the A. M. Obukhov Institute of Atmospheric Physics of the Russian Academy of Sciences [55, 56] for the scenario of anthropogenic impact of RCP8.5 with the increase in q_{CO_2} up to 1962 million⁻¹ by 2300 and the subsequent stabilization in 2301–3000. After that q_{CO_2} returns to pre-industrial value in accordance with one of the three scenarios (shown in different colors; the dependence of the results on the scenario of this return is low). The arrows show the direction of the climate trajectory.

6. EXAMPLES OF LINEAR AND NONLINEAR MECHANISMS OF THE EARTH SYSTEM RESPONSE FORMATION

6.1. Hysteresis-like phenomena in the Earth system

The presence of tipping points can contribute to partial irreversibility of the ongoing climate changes. According to the IPCC AR6 glossary, a change is considered irreversible on a given time scale if natural climatic processes cannot restore the original state on this time scale. Irreversibility is closely related to bifurcation tipping points and, in the case of multistability of the Earth climate system, to time scales of transition of the Earth climate from one steady state to another. This irreversibility manifests itself in the form of a hysteresis curve for climate variables.

The best-known example of such a hysteresis in climate is the dependence of the intensity of the oceanic conveyor on the intensity of the fresh water flow from the atmosphere (or land) to the North Atlantic (Sec. 5.3). Bistability of the system in a certain interval of values of this parameter leads to the fact that with an increase in the intensity and its subsequent decrease a hysteresis occurs [52]. Bistability of T_g also manifests itself in M. I. Budyko’s energy-balance climate model as the total solar irradiance change [41]. The climate characteristic hysteresis mechanism related to the multistability of the Earth system is fundamentally nonlinear.

Hysteresis-like curve for a number of climate characteristics also manifests itself in the development of a positive radiative forcing followed by a decrease to pre-industrial state [53, 54, 55, 56, 57, 58] (see also Fig. 4). In these calculations, the formation of the hysteresis curve is due to another mechanism, by virtue of which the time scale of one of the components of the Earth system significantly exceeds the effective time scale of inertia for the entire Earth system [55, 56, 58]. In connection with the latter, the term “transient hysteresis” was proposed for this mechanism in [55, 56]. This is a linear mechanism of climate hysteresis and irreversibility (in the above-mentioned sense) of the ongoing changes in the state of the Earth system.

Note that in [59] the response hysteresis is related to a combination of linear and nonlinear mechanisms: nonlinearity due to the interaction of climate and biogeochemical cycles leads to multistability, while the inertia of individual components of the Earth system ensures the slow development of instability.

6.2. Mutual delay between temperature and q_{CO_2}

According to ice core data for the last few hundred thousand years, paleoreconstructions for the last millennium and observational data for the end of the 20th century, a delay of the q_{CO_2} content variation relative to T_g was noted. This has been used as an argument to criticize anthropogenic causes of the current climate change (see review in [60, 61, 62]). However, such a delay was also obtained in numerical experiments with climate models, e. g., for the first half of the 19th century, when anthropogenic impact was relatively

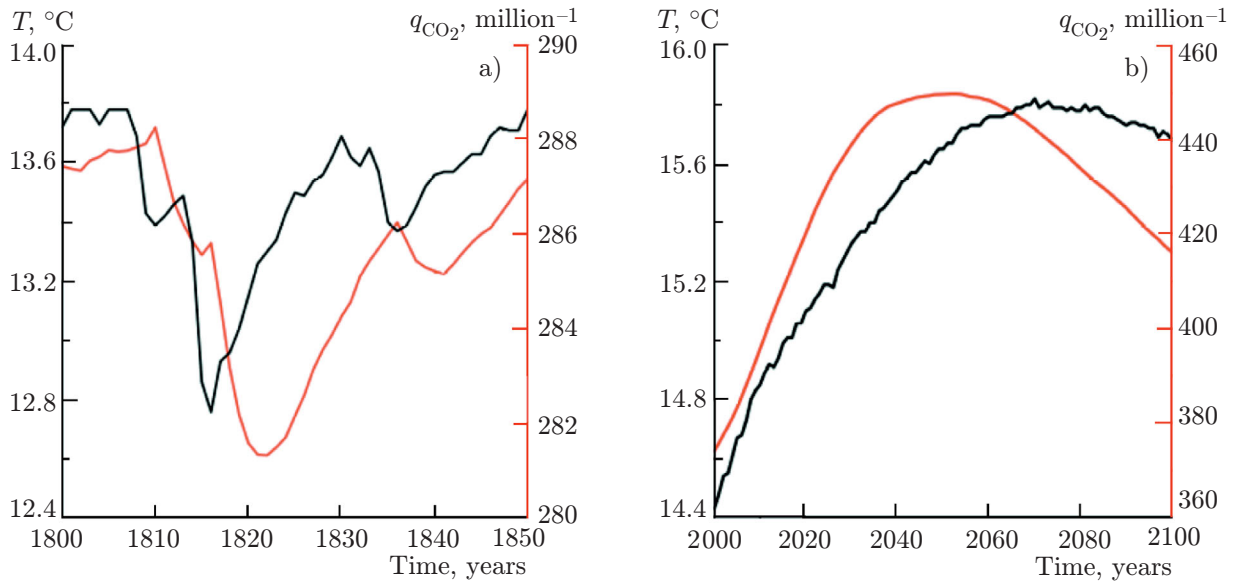


Fig. 5. Change in globally averaged annual surface temperature T_g (black lines, scales on the left) and CO_2 concentration in the atmosphere q_{CO_2} (orange lines, scales on the right) calculated using the Earth system model of the A. M. Obukhov Institute of Atmospheric Physics of the Russian Academy of Sciences [61, 62] for the first half of the 19th century (a) and for the 21st century under anthropogenic impact in accordance with the RCP2.6 scenario characterized by the maximum of q_{CO_2} in the middle of the 21st century (b).

small, but a number of large volcanic eruptions occurred (Fig. 5) [60, 61]. In model calculations for the 21st century with a significant anthropogenic impact the sign of such a delay changes to the opposite one. Thus, the indicated delay does not contradict the predominantly anthropogenic nature of the current climate change.

Note that the mechanism for the formation of such a delay, considered in [60, 61], is linear. This mechanism is related to the ratio of response time scales among q_{CO_2} , T_g , and other Earth system state variables. On the other hand, the corresponding nonlinear mechanism related to the nonlinear dependence of the greenhouse radiative forcing on q_{CO_2} is also possible. This mechanism manifests itself in the different signs of the delay between q_{CO_2} and T_g , depending on the direction of climate change, i.e., warming or cooling [62].

7. CONCLUSIONS

Thus, the following can be stated.

Climate change in the second half of the 20th century and in the first decades of the 21st century have been unprecedentedly fast. According to IPCC AR6, the current state of the climate is the warmest in the last 125 mln. years, and the current CO_2 concentration higher than in the last 2 mln. years.

The main cause of the current warming is anthropogenic activity (0.8–1.3 K of 0.95–1.20 K average for 2010–2019 relative to the average for 1850–1900), first of all, greenhouse gas emissions (1–2 K).

Globally, the climate response to radiative forcing is close to linear (the error does not exceed 10%). On smaller spatial scales, however, such a climate response is fundamentally nonlinear.

The nonlinearity of the response manifests itself in the dependence of the equilibrium climate sensitivity on the climate state, as well as the dependence of this sensitivity on time.

For individual processes, the formation of a climate response to external forcings is due to both linear and nonlinear mechanisms.

Nonlinear features of the climate response to external forcings may lead to the development of tipping points for the evolution of the climate system.

This work was supported by the Russian Science Foundation (project No. 21–17–00012). The author is grateful to V. A. Semenov and A. M. Feigin for useful discussions.

REFERENCES

1. V. Masson-Delmotte, P. Zhai, A. Pirani, et al., ed., *Climate Change 2021: The Physical Science Basis. Contribution of Working Group I to the Sixth Assessment Report of the Intergovernmental Panel on Climate Change*, Cambridge University Press, Cambridge/New York (2021).
2. M. Etminan, G. Myhre, E. J. Highwood, and K. P. Shine, *Geophys. Res. Lett.*, **43**, No. 24, 12614–12623 (2016). <https://doi.org/10.1002/2016GL071930>
3. M. E. Schlesinger and N. Ramankutty, *Nature*, **367**, No. 6465, 723–726 (1994). <https://doi.org/10.1038/367723a0>
4. C. Deser, M. A. Alexander, S.-P. Xie, and A. S. Phillips, *Ann. Rev. Mar. Sci.*, **2**, 115–143 (2010). <https://doi.org/10.1146/annurev-marine-120408-151453>
5. V. A. Semenov, M. Latif, D. Dommenges, et al., *J. Climate*, **23**, No. 21, 5668–5677 (2010). <https://doi.org/10.1175/2010JCLI3347.1>
6. X. Chen and K.-K. Tung, *Science*, **345**, No. 6199, 897–903 (2014). <https://doi.org/10.1126/science.1254937>
7. D. D. Bokuchava and V. A. Semenov, *Earth Sci. Rev.*, **222**, 103820 (2021). <https://doi.org/10.1016/j.earscirev.2021.103820>
8. N. P. Gillett, M. Kirchmeier-Young, A. Ribes, et al., *Nature Clim. Change*, **11**, No. 3, 207–212 (2021). <https://doi.org/10.1038/s41558-020-00965-9>
9. R. E. Benestad, D. Nuccitelli, S. Lewandowsky, et al., *Theor. Appl. Climatol.*, **126**, No. 3, 699–703 (2016). <https://doi.org/10.1007/s00704-015-1597-5>
10. A. G. Pendergrass, R. Knutti, F. Lehner, et al., *Sci. Rep.*, **7**, No. 1, 17966 (2017). <https://doi.org/10.1038/s41598-017-17966-y>
11. R. J. Stouffer and R. T. Wetherald, *J. Climate*, **20**, No. 21, 5455–5467 (2007). <https://doi.org/10.1175/2007JCLI1384.1>
12. E. D. Babina and V. A. Semenov, *Russ. Meteorol. Hydrol.*, **44**, No. 8, 513–522 (2019). <https://doi.org/10.3103/S1068373919080028>
13. E. D. Babina and V. A. Semenov, *Izv. Rossiisk. Akad. Nauk, Ser. Geogr.*, **86**, No. 4, 528–546 (2022). <https://doi.org/10.31857/S2587556622030049>
14. E. M. Volodin and A. S. Gritsun, *Atmos. Oceanic Phys.*, **56**, No. 3, 218–228 (2020). <https://doi.org/10.1134/S0001433820030123>
15. F. J. M. M. Nijse, P. M. Cox, and M. S. Williamson, *Earth Syst. Dyn.*, **11**, No. 3, 737–750 (2020). <https://doi.org/10.5194/esd-11-737-2020>
16. G. A. Meehl, C. A. Senior, V. Eyring, et al., *Sci. Adv.*, **6**, No. 26, eaba1981 (2020). <https://doi.org/10.1126/sciadv.aba1981>
17. G. Roe, *Annu. Rev. Earth Planet. Sci.*, **37**, 93–115 (2009). <https://doi.org/10.1146/annurev.earth.061008.134734>
18. I. M. Held and B. J. Soden, *J. Climate*, **19**, No. 21, 5686–5699 (2006). <https://doi.org/10.1175/JCLI3990.1>
19. G. L. Stephens, *J. Atmos. Sci.*, **35**, No. 11, 2111–2122 (1978). [https://doi.org/10.1175/1520-0469\(1978\)035\\$<2111:RPIEWC\\$>2.0.CO;2](https://doi.org/10.1175/1520-0469(1978)035$<2111:RPIEWC$>2.0.CO;2)

20. S. Bony and J.-L. Dufresne, *Geophys. Res. Lett.*, **32**, No. 20, L20806 (2005).
<https://doi.org/10.1029/2005GL023851>
21. S. C. Sherwood, M. J. Webb, J. D. Annan, et al., *Rev. Geophys.*, **58**, No. 4, e2019RG000678 (2020).
<https://doi.org/10.1029/2019RG000678>
22. C. Heinze, V. Eyring, P. Friedlingstein, et al., *Earth Syst. Dyn.*, **10**, No. 3, 379–452 (2019).
<https://doi.org/10.5194/esd-10-379-2019>
23. A. V. Eliseev, *Fundam. Prikl. Klimat.*, **4**, 9–31 (2017). <https://doi.org/10.21513/2410-8758-2017-4-9-31>
24. A. V. Eliseev, *Fundam. Prikl. Klimat.*, **1**, 52–70 (2018).
<https://doi.org/10.21513/2410-8758-2018-1-52-70>
25. J. Hansen, M. Sato, and R. Ruedy, *J. Geophys. Res.: Atmospheres*, **102**, No. D6, 6831–6864 (1997).
<https://doi.org/10.1029/96JD03436>
26. S. B. Fels, J. D. Mahlman, M. D. Schwarzkopf, and R. W. Sinclair, *J. Atmos. Sci.*, **37**, No. 10, 2265–2297 (1980). [https://doi.org/10.1175/1520-0469\(1980\)037<2265:SSTPIO>2.0.CO;2](https://doi.org/10.1175/1520-0469(1980)037<2265:SSTPIO>2.0.CO;2)
27. J. Hansen, M. Sato, R. Ruedy, et al., *J. Geophys. Res.: Atmospheres*, **110**, No. D18, D18104 (2005).
<https://doi.org/10.1029/2005JD005776>
28. I. I. Mokhov and M. G. Akperov, *Izv. Atmos. Oceanic Phys.*, **42**, No. 4, 430–438 (2006).
<https://doi.org/10.1134/S0001433806040037>
29. C. J. Smith, R. J. Kramer, G. Myhre, et al., *Geophys. Res. Lett.*, **45**, No. 21, 12023–12031 (2020).
<https://doi.org/10.1029/2018GL079826>
30. C. A. Senior and J. F. B. Mitchell, *Geophys. Res. Lett.*, **27**, No. 17, 2685–2688 (2000).
<https://doi.org/10.1029/2000GL011373>
31. K. D. Williams, W. J. Ingram, and J. M. Gregory, *J. Climate*, **21**, No. 19, 5076–5090 (2008).
<https://doi.org/10.1175/2008JCLI2371.1>
32. T. F. Stocker and S. J. Johnsen, *Paleoceanography*, **18**, No. 4, 1087 (2003).
<https://doi.org/10.1029/2003PA000920>
33. A. Schmittner, O. A. Saenko, and A. J. Weaver, *Quat. Sci. Rev.*, **22**, Nos. 5–7, 659–671 (2003).
[https://doi.org/10.1016/S0277-3791\(02\)00184-1](https://doi.org/10.1016/S0277-3791(02)00184-1)
34. A. Ganopolski and D. M. Roche, *Quat. Sci. Rev.*, **28**, Nos. 27–28, 3361–337 (2009).
<https://doi.org/10.1016/j.quascirev.2009.09.019>
35. M. Crucifix, *Geophys. Res. Lett.*, **33**, No. 18, L18701 (2006). <https://doi.org/10.1029/2006GL027137>
36. K. Meraner, T. Mauritsen, and A. Voigt, *Geophys. Res. Lett.*, **40**, No. 22, 5944–5948 (2013).
<https://doi.org/10.1002/2013GL058118>
37. J. E. Tierney, J. Zhu, M. Li, et al., in: *Proc. Nat. Acad. Sci.*, **119**, No. 42, e2205326119 (2022).
<https://doi.org/10.1073/pnas.2205326119>
38. T. Schneider, P. A. O’Gorman, and X. J. Levine, *Rev. Geophys.*, **48**, No. 3, RG3001 (2010).
<https://doi.org/10.1029/2009RG000302>
39. M. V. Kurgansky, *Theor. Appl. Climatol.*, **147**, Nos. 1–2, 65–71 (2022).
<https://doi.org/10.1007/s00704-021-03782-y>
40. P. Ashwin, S. Wiczorek, R. Vitolo, and P. Cox, *Philos. Trans. R. Soc., Ser. A*, **370**, No. 1962, 1166–1184 (2012). <https://doi.org/10.1098/rsta.2011.0306>
41. M. I. Budyko, *Climate Change* [in Russian], Gidrometeoizdat, Leningrad (1974).
42. A. M. Feigin and I. B. Kononov, *J. Geophys. Res.: Atmospheres*, **101**, No. D20, 26023–26038 (1996).
<https://doi.org/10.1029/96JD02011>

43. I. B. Konovalov, A. M. Feigin, and A. Y. Mukhina, *J. Geophys. Res.: Atmospheres*, **104**, No. D3, 3669–3689 (1999). <https://doi.org/10.1029/1998JD100037>
44. W. Steffen, J. Rockström, K. Richardson, et al., *Proc. Nat. Acad. Sci.*, **115**, No. 33, 8252–8259 (2018). <https://doi.org/10.1073/pnas.1810141115>
45. S. Bathiany, J. Hidding, and M. Scheffer, *J. Climate*, **33**, No. 15, 6399–6421 (2020). <https://doi.org/10.1175/JCLI-D-19-0449.1>
46. J. Zhu, Z. Liu, J. Zhang, and W. Liu, *Clim. Dyn.*, **44**, No. 11, 3449–3468 (2015). <https://doi.org/10.1007/s00382-014-2165-x>
47. V. V. Malakhova and A. V. Eliseev, *Glob. Planet. Change*, **157**, 18–25 (2017). <https://doi.org/10.1016/j.gloplacha.2017.08.007>
48. V. V. Malakhova and A. V. Eliseev, *Glob. Planet. Change*, **192**, 103249 (2020). <https://doi.org/10.1016/j.gloplacha.2020.103249>
49. V. Brovkin, E. Brook, J. W. Williams, et al., *Nature Geosci.*, **14**, No. 8, 550–558 (2021). <https://doi.org/10.1038/s41561-021-00790-5>
50. N. Wunderling, J. F. Donges, J. Kurths, and R. Winkelmann, *Earth Syst. Dyn.*, **12**, No. 2, 601–619 (2021). <https://doi.org/10.5194/esd-12-601-2021>
51. P. D. L. Ritchie, J. J. Clarke, P. M. Cox, and C. Huntingford, *Nature*, **592**, No. 7855, 517–523 (2021). <https://doi.org/10.1038/s41586-021-03263-2>
52. S. Rahmstorf, M. Crucifix, A. Ganopolski, et al., *Geophys. Res. Lett.*, **32**, No. 23, L23605 (2005). <https://doi.org/10.1029/2005GL023655>
53. D. M. Lawrence and A. G. Slater, *Geophys. Res. Lett.*, **32**, No. 24, L24401 (2005). <https://doi.org/10.1029/2005GL025080>
54. O. Boucher, P. R. Halloran, E. J. Burke, et al., *Environ. Res. Lett.*, **7**, No. 2, 024013 (2012). <https://doi.org/10.1088/1748-9326/7/2/024013>
55. A. V. Eliseev, P. F. Demchenko, M. M. Arzhanov, and I. I. Mokhov, *Dokl. Earth Sci.*, **444**, No. 2, 725–728 (2012). <https://doi.org/10.1134/S1028334X12060025>
56. A. V. Eliseev, P. F. Demchenko, M. M. Arzhanov, and I. I. Mokhov, *Clim. Dyn.*, **42**, Nos. 5–6, 1203–1215 (2014). <https://doi.org/10.1007/s00382-013-1672-5>
57. P. Wu, J. Ridley, A. Pardaens, et al., *Clim. Dyn.*, **45**, No. 3, 745–754 (2016). <https://doi.org/10.1007/s00382-014-2302-6>
58. S.K. Kim, J. Shin, S.-I. An, et al., *Nature Clim. Change*, **12**, No. 9, 834–840 (2022). <https://doi.org/10.1038/s41558-022-01452-z>
59. P. de Vrese and V. Brovkin, *Nature Commun.*, **12**, No. 1, 2688 (2021). <https://doi.org/10.1038/s41467-021-23010-5>
60. K. E. Muryshev, A. V. Eliseev, I. I. Mokhov, and A. V. Timazhev, *Dokl. Earth Sci.*, **463**, No. 2, 863–867 (2015). <https://doi.org/10.1134/S1028334X15080231>
61. K. E. Muryshev, A. V. Eliseev, I. I. Mokhov, and A. V. Timazhev, *Glob. Planet. Change*, **148**, 29–41 (2017). <https://doi.org/10.1016/j.gloplacha.2016.11.005>
62. K. E. Muryshev, A. V. Eliseev, I. I. Mokhov, et al., *Dokl. Earth Sci.*, **501**, No. 1, 949–954 (2021). <https://doi.org/10.1134/S1028334X21110118>